Dalton Transactions

RSC Publishing

PAPER

View Article Online
View Journal | View Issue

Cite this: *Dalton Trans.*, 2013, **42**, 13923

Reactions of Cp_2M (M = Ni, V) with dilithium diamido-aryl reagents; retention and oxidation of the transition metal ions†

Francesca A. Stokes,[a] Mark A. Vincent,[b] Ian H. Hillier,[b] Tanya K. Ronson,[a] Alexander Steiner,[c] Andrew E. H. Wheatley,*[a] Paul T. Wood[a] and Dominic S. Wright*[a]

Received 19th June 2013,
Accepted 27th July 2013

DOI: 10.1039/c3dt51632f

www.rsc.org/dalton

The reactions of dilithium 1,2-diamidobenzene, $[1,2\text{-}(HN)_2C_6H_4]Li_2$ ($\mathbf{L^1H_2}$)Li_2, and dilithium 1,8-diamidonaphthalene, $[1,8\text{-}(NH)_2C_{10}H_6]Li_2$ ($\mathbf{L^2H_2}$)Li_2, with Cp_2Ni and Cp_2V have been used to obtain the new complexes ($\mathbf{L^2H_2}$)$_2$Ni{Li(THF)$_2$}$_2$ (**3**), ($\mathbf{L^2H_2}$)$_3$V{Li(THF)$_2$}$_3$ (**4**) and ($\mathbf{L^1H_2}$)$_6$Ni$_6$·{[($\mathbf{L^1H_2}$)$_3$($\mathbf{L^1H}$)$_3$Ni$_6$Li(THF)]$^{2-}$·2[Li(THF)$_4$]$^+$} (**5**), in which retention or oxidation of the initial metal(II) centre is observed. Whereas **3** and **4** contain one transition metal ion within ion-paired structures, **5** has a complicated co-crystalline composition which contains octahedral Ni$_6$-cages constructed from six square-planar (16e) Ni^{II} centres.

Introduction

In contrast to ferrocene (Cp_2Fe), in which the Cp–Fe interactions are predominantly covalent, the other first-row metallocenes are far more polar. As a result, these species have extensive synthetic utility as sources of the metal atoms in a range of organometallic and metallo-organic compounds. Extensive synthetic studies involving a broad range of N-, O- and C-based organic acids and nucleophiles have identified three main types of reactivity; (*i*) the deprotonation of organic acids (RH) by the anionic Cp ligands (*pathway 1*, Scheme 1),[1] (*ii*) the addition of weaker nucleophiles (R^-) to the transition metal centre (M) without displacement of the Cp ligands (*pathway 2*),[2] and (*iii*) nucleophilic displacement of the Cp^- ligands by stronger heteroatomic and organometallic nucleophiles (R^-) (*pathway 3*).[3] A common feature of all of these reactions is that the +2 oxidation state of the transition metal ion is maintained throughout, so that Cp_2M has functioned as an organically-soluble source of M^{2+} ions.

The ability to maintain the oxidation state of the transition metal in the course of each of the reactions in Scheme 1 is of particular interest in the formation of multiply-bonded transition metal compounds in which the retention of a low oxidation state is important for the participation of the metal d-orbitals in bonding. Some of our most recent studies have shown that the use of Cp_2M (M = V, Cr, Mn, Ni) as metal precursors can indeed lead to formally multiply-bonded transition metal compounds. For example, the reaction of (hpp)Li (hppH = 1,3,4,6,7,8-hexahydro-2*H*-pyrimido[1,2,*a*]pyrimidine) with Cp_2V gives the remarkable complex [{V_2(hpp)$_4$}Li(μ^5-Cp)Li(μ^5-Cp)Li{V_2(hpp)$_4$}]$^+$·[(η^5-Cp)Li(η^5-Cp)Li(η^5-Cp)]$^-$ in which a V≡V triply-bonded fragment V_2(hpp)$_4$[3c] functions as a metal-based Lewis base ligand in the trapping of a [{V_2(hpp)$_4$}Li(μ^5-Cp)Li(μ^5-Cp)Li{V_2(hpp)$_4$}]$^+$ cation.[2] Meanwhile, whereas reaction of the sterically-undemanding lithium amidinate [MeN···C(H)···NMe]Li with Cp_2Cr has given the classical, lantern-shaped compound Cr_2[MeN···C(H)···NMe]$_4$, which contains a Cr–Cr quadruple bond,[3d] the use of the dilithiate of 2,3-diphenyl guanidine [(PhNH)$_2$C=NH = $\mathbf{LH_3}$] gives [Cr_2($\mathbf{LH}$)$_4$]{Li(THF)$_2$}$_4$(LiCp)$_2$, which contains a quadruply-bonded Cr^{II} tetraanion.[3]

Most recently, however, it was found that the tendency to maintain the metal +2 oxidation state in these reactions may

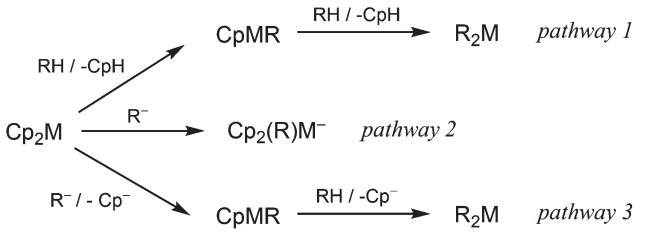

Scheme 1 Common reactivity patterns of polar metallocenes with organic acids and nucleophiles.

[a]*Department of Chemistry, University of Cambridge, Lensfield Road, Cambridge, CB2 1EW, UK. E-mail: aehw2@cam.ac.uk, dsw1000@cam.ac.uk; Fax: +44 (0)1223 336362; Tel: +44 (0)1223 763966*
[b]*School of Chemistry, The University of Manchester, Manchester, M13 9PL, UK*
[c]*Department of Chemistry, University of Liverpool, Crown street, Liverpool, L69 7ZD, UK*

†Electronic supplementary information (ESI) available: DFT coordinates for **5a** and **5b**$^{2-}$. CCDC 943106–943108. For ESI and crystallographic data in CIF or other electronic format see DOI: 10.1039/c3dt51632f

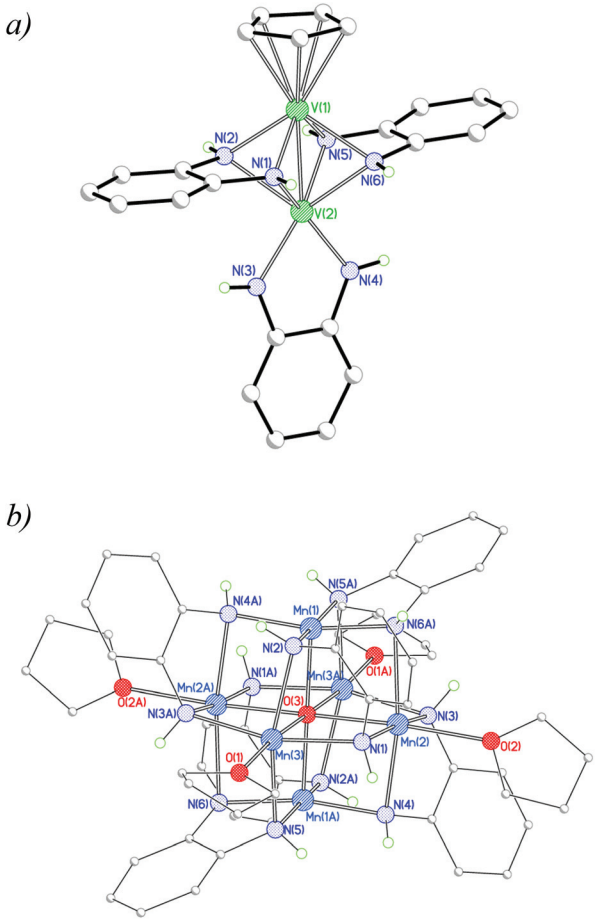

Fig. 1 (a) Structure of the V^{III} $[(\eta^5\text{-Cp})(\mathbf{L^1H_2})_2VV(\mathbf{L^1H_2})]^-$ anionic component of **1** and (b) the $Mn^{II}_4Mn^{III}_2$ cage **2**.

be far more dependent on the particular organic acid or nucleophile employed than had been realised in earlier studies. The potential for complicated redox behaviour of the dianion of 1,2-diaminobenzene, $[1,2\text{-}(HN)_2C_6H_4]^{2-}$ ($\mathbf{L^1H_2}$), had already been observed in a number of main group[4] and transition metal reactions.[5] For example, the reaction of dilithium 1,2-diamidobenzene, $[1,2\text{-}(HN)_2C_6H_4]Li_2$ $(\mathbf{L^1H_2})Li_2$ with the Sn^{II} base $Sn(NMe_2)_2$ is known to result in the formation of a mixed oxidation state Sn^{II}/Sn^{IV} complex.[4] With this behaviour in mind we have begun to explore the reactions of $(\mathbf{L^1H_2})Li_2$ with metallocene. We found that the reactions with Cp_2V and Cp_2Mn gave the V^{III} complex $[(\eta^5\text{-Cp})(\mathbf{L^1H_2})_2VV(\mathbf{L^1H_2})]^-$-$[Li(THF)_4]^+$ (**1**) (Fig. 1a)[6] and the oxo-capture $Mn^{II}_4Mn^{III}_2$ cage $Mn_6(\mathbf{L^1H_2})_6(\mu_6\text{-O})(THF)_4$ (**2**) (Fig. 1b), respectively,[6] in which (unlike in all other reactions of Cp_2M observed so far) the metal centres are oxidised or partially oxidised during the course of reaction.

We present here further synthetic and structural studies involving the reactions of Cp_2Ni and Cp_2V with dilithium 1,2-diamidobenzene, $[1,2\text{-}(HN)_2C_6H_4]Li_2$ $(\mathbf{L^1H_2})Li_2$, and related dilithium 1,8-diamidonaphthalene, $[1,8\text{-}(NH)_2C_{10}H_6]Li_2$ $(\mathbf{L^2H_2})$-Li_2, in which we have explored the potential for (*i*) redox chemistry in these systems and (*ii*) molecular aggregation.

Results and discussion

Solid-state and solution studies

Initial reactions focused on use of the 1,8-diaminonaphthalene ($\mathbf{L^2H_4}$). This was doubly deprotonated by its reaction with 2 equivalents of ^{n}BuLi in THF solution. Slow addition of the dilithiate, $(\mathbf{L^2H_2})Li_2$, to a solution of Cp_2Ni or Cp_2V (1 equivalent) at −78 °C gave dark red and dark yellow solutions, respectively, from which the new compounds $(\mathbf{L^2H_2})_2Ni\{Li(THF)_2\}_2$ (**3**) and $(\mathbf{L^2H_2})_3V\{Li(THF)_2\}_3$ (**4**) were isolated in crystalline form (Scheme 2) (in 34 and 6% crystalline yields, respectively). Both compounds were characterised by ^1H and ^{13}C NMR spectroscopy and by elemental (C, H, N) analysis prior to obtaining their single-crystal X-ray structures. Although both complexes proved insoluble in most organic solvents (toluene, benzene and THF), the ^1H NMR spectra of **3** and **4** could be obtained in DMSO-d_6 at room temperature and showed the presence of a single environment for the $\mathbf{L^2H_2}$ ligands and a 2 : 1 ratio of THF : $\mathbf{L^2H_2}$, which is consistent with the later structural characterisation of the complexes. Although no N–H resonance was observed in the ^1H NMR spectrum of **4** at room temperature, the spectrum of **3** exhibited an N–H resonance at δ 1.36. The integration of this signal with respect to the aromatic resonances (in the region δ 5.26–6.12) showed that double deprotonation of the $\mathbf{L^2H_4}$ precursor had occurred.

The low-temperature single-crystal structures of **3** and **4** show that molecules of both contain only a single transition metal atom. This contrasts with recent studies of the reactions of Cp_2V and Cp_2Cr with related ligands which give singly- or multiply-bonded $(metal)_2$ compounds.[1–3,6] In the case of **3**, the structure consists of a central distorted square-planar Ni^{II} ion that is bonded to the four N-donor atoms of two dianionic $\mathbf{L^2H_2}$ ligands (Ni(1)–N(1) 1.876(2), Ni(1)–N(2) 1.900(2) Å; N(1)–Ni(1)–N(2) 94.54(11), N(1)–Ni(1)–N(2A) 85.46(11)°). These N-atoms are, in turn, bonded to two symmetry-related, THF-solvated Li^+ cations on either side of the centrosymmetric structure of **3**. The asymmetry with the $\mathbf{L^2H_2}$ dianions bond to the central Ni(II) atom is not discernable in the corresponding

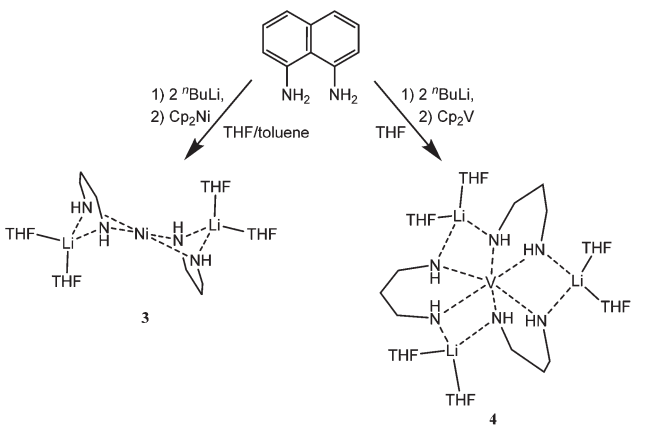

Scheme 2 Reactions producing **3** and **4**. The naphthalene ring systems in the products have been omitted for clarity.

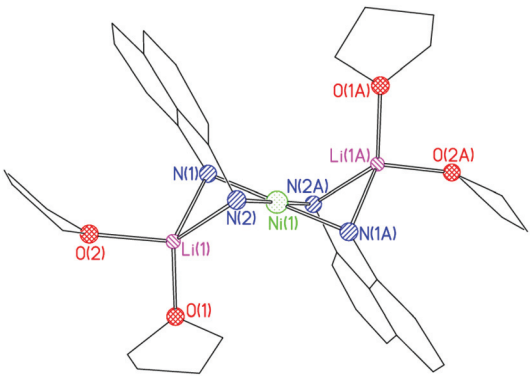

Fig. 2 Molecular structure of **3**. H-atoms are omitted for clarity. Selected bond lengths (Å) and angles (°); Ni(1)–N(1) 1.876(2), Ni(1)–N(2) 1.900(2), Li(1)–N(1) 2.081(5), Li(1)–N(2) 2.100(5). Ni(1)···Li(1) 2.554(5), N(1)–Ni(1)–N(2) 94.54(11), N(1)–Ni(1)–N(2A) 85.46(11), Ni(1)–N(1)–Li(1) 80.20(17), Ni(1)–N(2)–Li(1) 79.19(17).

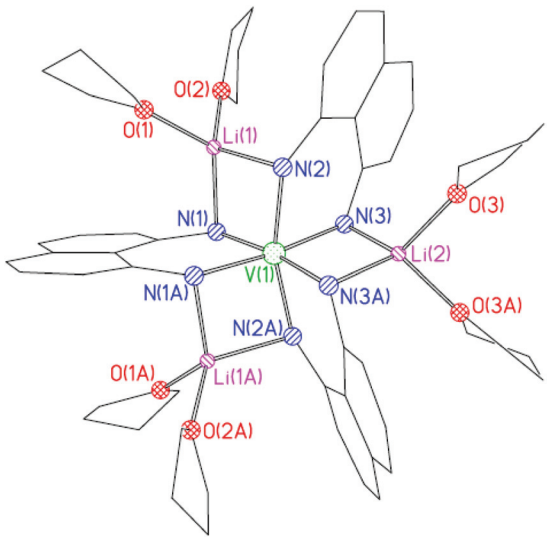

Fig. 3 Structure of the core of **4**. H-atoms omitted for clarity. Selected bond lengths (Å) and angles (°); V(1)–N 2.047(2)–2.094(3), V(1)···Li 2.741(9)–2.792(5), N–Li 2.068(6)–2.117(6), Li–O 1.931(6)–1.959(6), N–V–N 82.4(1)–97.5(1), N–Li–N 93.5(2)–98.4(4).

Li–N bond lengths (Li(1)–N(1) 2.081(5), Li(1)–N(2A) 2.100(5) Å), which are each as expected for essentially ionic Li–N interactions.[7] Significant puckering is seen in the LiN_2Ni ring units along the N(1)···N(2) vector (the puckering angle being *ca.* 115°). Overall, the structure of **3** is best regarded as an ion-paired complex of the $[Ni(\mathbf{L^2H_2})_2]^{2-}$ dianion with two THF-solvated Li^+ cations.

A number of compounds containing the dianionic $\mathbf{L^2H_2}$ ligand have been structurally characterised previously, and the $\kappa^{1,2}N$-$\kappa^{1,2}N'$-bridging mode found in **3** has been seen in several dinuclear transition metal compounds (Fig. 2).[8] Additionally, there exist examples of heterometallic transition metal/main group metal complexes in which 1,8-*N*-alkylated or -silylated naphthylamido ligands bridge the metal centres, examples being the Mn^{II}/Li complex (THF)Mn(Cl){1,8-$(Me_3SiN)_2C_{10}H_6$}-Li(THF)[9] and the Tl^{I}/Li complex Tl{1,8-$(Me_3SiN)_2C_{10}H_6$}-$Li(THF)_2$,[10] both of which incorporate the $\kappa^{1,2}N$-$\kappa^{1,2}N'$-ligand mode to bridge the metals centres.

The solid-state structure of **4** (Fig. 3) shows that the complex consists of a $[V(\mathbf{L^2H_2})_3]^{3-}$ anion that is coordinated by three $[Li(THF)_2]^+$ cations using a similar ligand bridging mode to that in **3** (now, however, with each of the ligand N-atoms bonding to separate Li^+ ions). While the oxidation state of the Ni^{II} centre (unsurprisingly) remained unchanged in the formation of **3**, the V^{II} centre present in the Cp_2V starting material has been oxidised to V^{III} in the case of **4**. This is a similar outcome to that found in the formation of **1**, discussed in the introduction (Fig. 1a).[6]

In contrast to the structure of **1**, the $\mathbf{L^2H_2}$ ligands in **4** are essentially symmetrically bound to the central metal ion with the V–N bond lengths being normal for such interactions (V(1)–N(1) 2.054(3), V(1)–N(2) 2.047(2), V(1)–N(3) 2.094(3) Å).[7] The V^{III} ion adopts a distorted octahedral geometry (N(1)–V(1)–N(2) 97.46(10), N(3)–V(1)–N(3A) 96.78(15)°). Whereas puckered four-membered LiN_2Ni metallocyclic units were noted in **3**, the three LiN_2V ring units in **4** are essentially planar (being puckered along the Li(1)···V(1) vector by no more than *ca.* 171°). Although complexes containing octahedral V^{III} ions are known for a range of ligands,[11] complexes containing octahedral V^{III} which are tris-coordinated by chelating anionic N-ligands are relatively rare and **4** is the first example of a transition metal complex of the type $[(\mathbf{L^2H_2})_3M]^{n+}$ (or indeed of any anionic N-ligand related to $\mathbf{L^2}$).

Following on from our initial studies of the reactions using the 1,2-benzenediamine ($\mathbf{L^1H_4}$) framework with Cp_2Mn and Cp_2V, in which oxidation or partial oxidation of the metal centres was observed,[6] the dilithium salt $(\mathbf{L^1H_2})Li_2$ (prepared *in situ* by the reaction of $\mathbf{L^1H_4}$ with 2 equivalents of ^{n}BuLi) was reacted with Cp_2Ni (2 : 1 equivalents, respectively) under N_2 at −78 °C in THF. Subsequent storage of the reaction mixture at room temperature afforded highly air-sensitive purple crystals of a new complex, **5** (67% with respect to Cp_2Ni), which exhibits a complicated co-crystalline structure in the solid state (Scheme 3).

The single crystal X-ray diffraction study of **5** reveals an extensively disordered structure comprising a 1 : 1 co-crystalline mixture of two closely related octahedral Ni^{II}_6 cages, $(\mathbf{L^1H_2})_6Ni_6$ cage (**5a**) (Fig. 4a) (solely containing the doubly-deprotonated $[C_6H_4(NH)_2]^{2-}$ ligand) and $[(\mathbf{L^1H_2})_3(\mathbf{L^1H})_3Ni_6Li(THF)]^{2-}\cdot 2[Li(THF)_4]^+$ **5b**$\cdot 2[Li(THF)_4]$ (the dianionic part of which, $\mathbf{5b^{2-}}$, is shown in Fig. 4b and which contains a mixture of doubly-deprotonated $[C_6H_4(NH)_2]^{2-}$ and triply-deprotonated $[C_6H_4(NH)(N)]^{3-}$ ligands). In addition, there are several molecules of THF within the lattice, one of which forms a close contact to Ni(5) (*ca.* 2.55 Å) (solvent not shown in Fig. 4a). Triple deprotonation of $\mathbf{L^1H_4}$ has been observed previously only in its reaction with the superbase mixture Sn-$(NMe_2)_2$/^{n}BuLi.[4]

The crystallographic model for **5** is based on multiple data collections using conventional X-ray analysis as well as

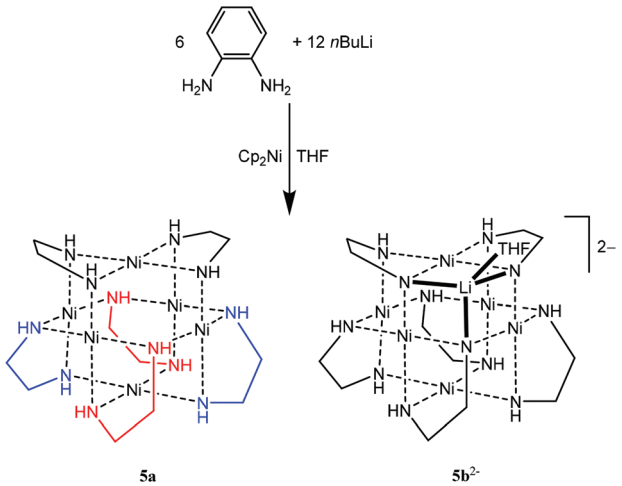

Scheme 3 Formation of the two types of Ni_6 cage arrangement, **5a** and $\mathbf{5b^{2-}}$, obtained by the reaction of $(\mathbf{L^1H_2})Li_2$ with Cp_2Ni. The three environments of the ligand backbones present in **5a** are coloured black, red and blue.

synchrotron radiation, all of which indicated the same ratio of **5a** to **5b**·2[Li(THF)$_4$]. Despite the high R_1 value of 14.3% (obtained using synchrotron radiation), which ostensibly results from subtle structural variations between the neutral and dianionic Ni_6 cages **5a** and $\mathbf{5b^{2-}}$, the identity and essential connectivity of the separate cage components are not in doubt. Moreover, this formulation is also consistent with elemental C, H and N analysis on the bulk sample.

The unusual cubeoctahedral arrangement of six, square-planar Ni^{II} ions and twelve N-atoms found in **5** is similar to the structure of the hexanuclear complex $[Ni(NH_2)_2]_6$,[12] and structurally equivalent to $(PtCl_2)_6$.[13] Ni_6 octahedra have also been observed in the cluster complex $(CpNi)_6$[14] and hexanuclear, heteroatom-bridged cages such as $Ph_3PNi_6Se_5$.[15] Although within the range of potential Ni–Ni bonds,[7] the Ni···Ni contacts within the core of **5** (range 2.74–2.82 Å; *cf.* 2.83 Å in $[Ni(NH_2)_2]_6$ [12]) are unlikely to represent bonding interactions and it seems more appropriate to regard this cage within the context of conventional square-planar Ni^{II} (d^8) coordination compounds. It can be noted in this regard that the Ni^{II} centres in **5** each have the expected 16e count.

In contrast to the straightforward spectroscopic analyses of **3** and **4** (see Experimental section) compound **5** exhibited complicated behaviour in the aromatic region of the ^{1}H NMR spectrum in a variety of solvents (DMSO-d_6, C_5H_5N-d_5, THF-d_8). Three different types of aromatic rings are clearly discernible in a 1 : 1 : 1 ratio by a combination of ^{1}H NMR and COSY (in DMSO-d_6, in which **5** is most soluble). This conclusion is reenforced by HMBC NMR spectroscopy (in DMSO-d_6) which indicates that three types of $\mathbf{L^1H_2}$ ligand are present in solution in equal abundance and allows the assignment of each of the NH groups to their respective C_6H_4 ring units (Fig. 5a and 5b). The observation of six distinct NH groups of equal integral at very high field (δ 0.63 to −2.10) is consistent with only the neutral cage **5a** being present in DMSO. The highly reactive cage $\mathbf{5b^{2-}}$ is presumably completely converted into **5a** *via* the

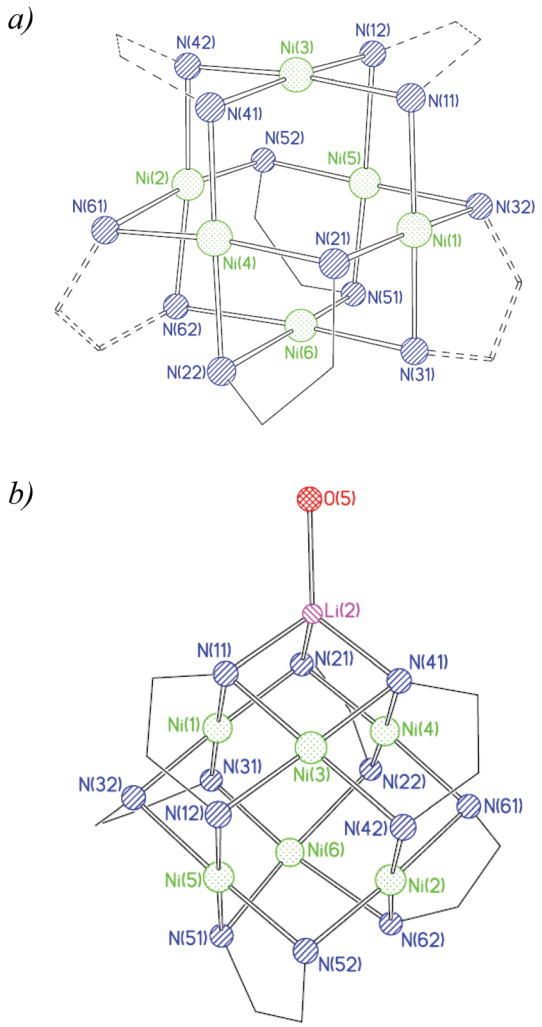

Fig. 4 (a) The structure of **5a** with the three types of chelating ligand highlighted (H-atoms and aromatic rings excluded) and (b) structure of the anion $\mathbf{5b^{2-}}$ incorporating its Li(THF) component (showing only the O-atom of THF, and with H-atoms and aromatic rings and the two $[Li(THF)_4]^+$ counter-ions omitted for clarity).

protonation reaction $\mathbf{5b^{2-}} + 3H^+ \rightarrow$ **5a**; a reaction which is not unexpected given the known relatively high acidity of the Me-groups of DMSO compared to potent bases such as, for example, organolithium reagents.[16]

Theoretical studies

To complement our experimental studies, density functional theory (DFT) calculations were carried out on **5a** and $\mathbf{5b^{2-}}$ using Gaussian 09.[17] The structures of both species were optimized for the $S = 0$ spin state using the M06-L and a 6-31+G** basis. This functional was chosen for its computational efficiency and has previously been shown to be suitable for describing metal clusters.[18] The predicted structures of these species along with important inter-atomic distances are shown in Fig. 6. In the case of **5a**, the predicted Ni···Ni and Ni–N lengths which span 2.74–2.91 and 1.93–1.99 Å, respectively, are

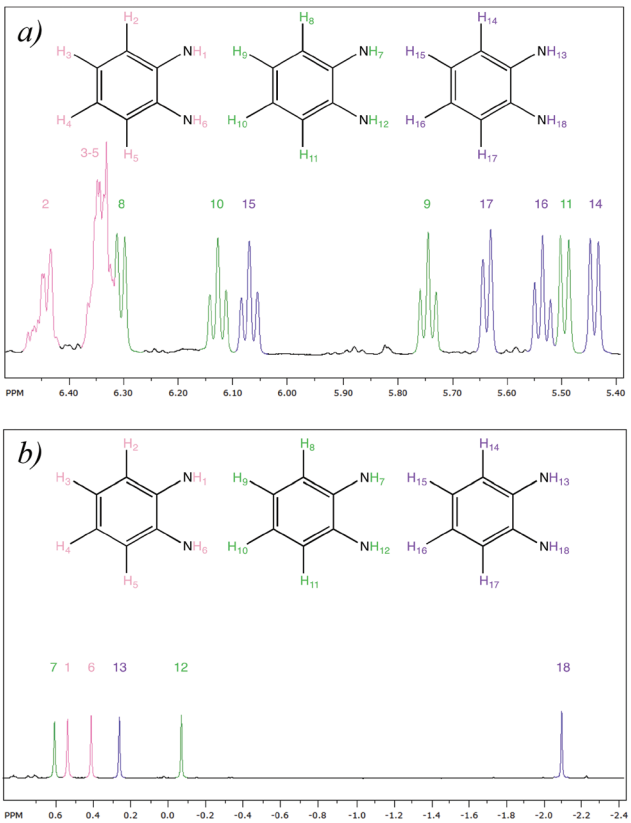

Fig. 5 The ^{1}H NMR spectrum of **5**; (a) the aromatic region and (b) the N–H region. The assignments are indicated by colour.

in good agreement with our X-ray findings. Interestingly, **5a** is predicted to have a significant electron affinity (153 kJ mol^{-1}) so that in the solid state, electron transfer from **5b**$^{2-}$ could well modify the geometric and electronic structure of the cluster. Moreover, when **5a** is deprotonated we find that the energy of the HOMO of **5a**$^-$ is negative, implying that this species does not readily undergo electron loss and that it thus represents the first step in the formation of **5b**$^{2-}$.

We subsequently used the computed structure of **5a** to predict the corresponding ^{1}H NMR chemical shifts using the Gauge Independent Atomic Orbital (GIAO) method in conjunction with both the B3LYP and M06-L functionals and a large basis set (6-311++G(2df,2pd)). We have also investigated the effect of solvent (DMSO), which has been included by a continuum (bulk) model (SMD), on the M06-L ^{1}H NMR spectroscopic shifts. We find that the aromatic signals are predicted to fall in the range δ 6.84–6.21 and δ 6.89–6.13 for the B3LYP and M06-L functionals, respectively. These data are in reasonable agreement with the experimentally observed range of δ 6.45–5.45. The predicted chemical shifts of the twelve NH groups (six pairs in C_2 symmetry) are shown in Table 1, and are to be compared to the experimental spectrum, which has five peaks in the range δ 0.63 to −0.05 with a sixth peak well separated at δ −2.10. According to the calculations, and in line with expectation, the hydrogen atoms are all protic rather than hydridic in nature. B3LYP and initial M06-L calculations

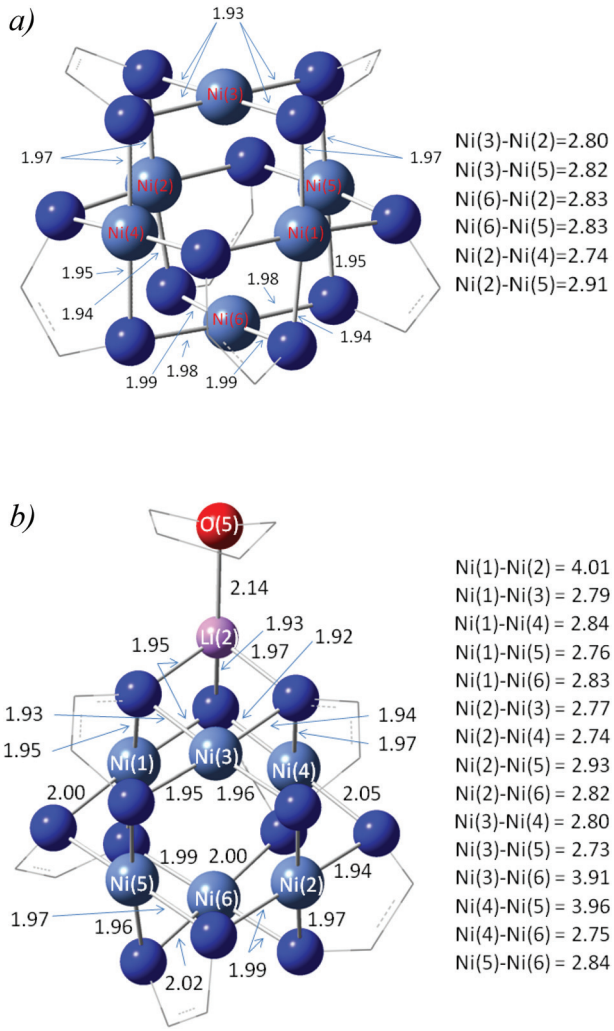

Fig. 6 Structures of (a) **5a** and (b) **5b**$^{2-}$ at the M06-L/6-31+G** level.

Table 1 ^{1}H NMR spectroscopic shifts (ppm) for **5a** calculated using the B3LYP and M06-L functional

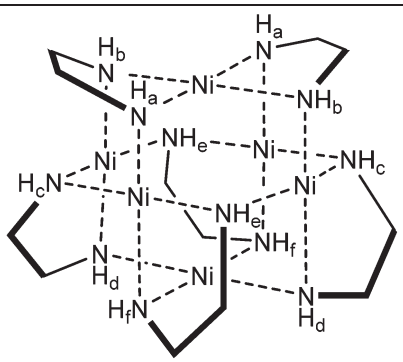

	H_a	H_b	H_c	H_d	H_e	H_f
B3LYP	−1.98	−1.73	−3.12	−2.91	−2.14	−2.71
M06-L	+0.69	+0.94	−0.60	−0.61	+0.78	−0.43
M06-L[a]	+1.59	+1.85	−0.52	−0.01	+1.70	+0.02

[a] With bulk solvent (DMSO) modelled by SMD method.

reported in Table 1 (lines 1 and 2) predict the same general pattern of two groups (H_a, H_b, H_e and H_c, H_d, H_f) of three fairly closely spaced lines, and thus do not reproduce the experimentally observed pattern of shifts well. However, we can see from the geometric structure that due to their close proximity to the face of the aromatic rings, $H_{c/d/f}$ are shielded from solvent to a greater extent than are $H_{a/b/e}$. This should be reflected in the effect of solvent on the calculated chemical shifts and, in line with this, the overall spread of the NH resonances is increased when the SMD method is used. Hence, the inclusion of solvent effects in the calculations raises the spread of the computed NH resonances from a value of δ 1.55 (Table 1, line 2) to one of δ 2.37 (Table 1, line 3), bringing it significantly closer to the experimentally seen spread of δ 2.73 (see above). Moreover, in addition to giving an improved range of computed shifts, the inclusion of solvent effects starts to distinctly separate one high-field NH (H_c) from the other peaks – again in line with experimental observation.

Conclusions

The combined studies of the reactions of Cp_2M (M = V, Mn, Ni) with the related amido-aryl salts $(\mathbf{L^1H_2})Li_2$ and $(\mathbf{L^2H_2})Li_2$ reported by us in our previous communication[6] and in the current paper reveal that retention or increase of the transition metal oxidation state can occur depending on the transition metal present in the precursor. Whereas V and Mn show partial or complete oxidation of the metal centres with this type of ligand, Ni proves to be considerably more redox stable. The mechanism and associated redox chemistry involved in these systems is not currently understood. However, the use of $\mathbf{L^1H_2}$ and $\mathbf{L^2H_2}$ as supporting ligands clearly has the capacity to yield high nuclearity transition metal complexes. In the current study this feature is seen through formation of the Ni_6 compound **5**.

Experimental section

Synthesis

All reactions were performed under dry, O_2-free N_2. Solvents (THF and toluene) were dried using Na/benzophenone. Products were handled and stored in a glove box (Saffron, type β). Cp_2Ni and Cp_2V were obtained using literature procedures and were purified by sublimation.[19,20] ^{n}BuLi in hexanes was acquired from Aldrich and was used without standardising. NMR spectra were recorded on a Bruker DRX 500 FT-NMR spectrometer using deuterated NMR solvents (THF-d_8 and C_5H_5N-d_5 were dried using a Na mirror, DMSO-d_6 was used as supplied). ^{1}H and ^{13}C NMR spectra were referenced to the solvent peaks. ^{7}Li NMR spectra were referenced to 1 M LiOH–D_2O. Elemental analysis (C, H and N) was obtained in-house using an Exeter Analytical CE-440 Elemental Analyzer.

Synthesis of 3. 1,8-Diaminonaphthalene (87 mg, 0.55 mmol) was dissolved in 5 mL of THF. ^{n}BuLi (0.7 mL, 1.6 mol L^{-1} in hexanes, 1.10 mmol) was syringed into this solution dropwise under N_2 at −78 °C. A solution of Cp_2Ni (100 mg, 0.55 mmol) in 5 mL toluene was cooled to −78 °C and the ligand solution added to this dropwise by syringe. The resulting dark red solution was allowed to warm to room temperature. It was stirred overnight before being filtered while warm. Storage at −30 °C afforded highly air-sensitive orange-red crystals in a dark red solution. Yield 125 mg, 34% with respect to Cp_2Ni. Melting point, did not melt up to 360 °C. ^{1}H NMR (500.05 MHz, DMSO-d_6), δ (ppm) = 6.12 (4H, t, $^3J_{H-H}$ = 7.61 Hz, *m*-CH), 5.41 (4H, d, $^3J_{H-H}$ = 7.36 Hz, *p*-CH), 5.26 (4H, d, $^3J_{H-H}$ = 7.54 Hz, *o*-CH), 3.58 (16H, m, THF CH_2O), 1.74 (16H, m, THF CH_2), 1.36 (4H, m, N–H). ^{13}C NMR (125.8 MHz, THF-d_8), δ (ppm) = 155.6 (HN*C*), 140.4 (CH*C*CH), 126.4 (CH*C*HCH), 117.3 (NHC*C*CNH), 102.5 (HN*C*CH), 101.8 (CH*C*HC), 67.5 (THF *C*H_2O), 25.6 (THF *C*H_2). Elemental analysis – found C 64.3, H 7.2, N 8.7, cald. for $C_{40}H_{34}Li_2N_8Ni_2O_4$ C 64.2, H 7.2, N 8.3.

Synthesis of 4. 1,8-Diaminonaphthalene (87 mg, 0.55 mmol) was dissolved in 5 mL of THF. ^{n}BuLi (0.7 mL, 1.6 mol L^{-1} in hexanes, 1.10 mmol) was syringed into this solution dropwise under N_2 at −78 °C. A solution of Cp_2V (100 mg, 0.55 mmol) in 5 mL THF was cooled to −78 °C and the ligand solution added to this dropwise by syringe. The resulting dark yellow solution was allowed to warm to room temperature. It was stirred overnight before being filtered while warm. Storage of the filtrate at 4 °C afforded highly air-sensitive brown crystals in a dark solution. Yield 30 mg, 6% with respect to Cp_2V. Melting point, 161–164 °C. ^{1}H NMR (500.05 MHz, DMSO-d_6), δ (ppm) = 6.35 (6H, t, $^3J_{H-H}$ = 7.64 Hz, *m*-CH), 5.74 (6H, d, $^3J_{H-H}$ = 7.72 Hz, *p*-CH), 5.42 (6H, d, $^3J_{H-H}$ = 7.65 Hz, *o*-CH), 3.60 (m, THF CH_2O), 1.76 (m, THF CH_2) (N–H not observed). ^{13}C NMR (125.8 MHz, THF-d_8), δ (ppm) = 154.5 (HN*C*), 145.3 (CH*C*CH), 131.3 (CH*C*HCH), 131.2 (NHC*C*CNH), 110.0 (HNC*C*H), 109.9 (CH*C*HC), 72.3 (THF, *C*H_2O), 30.4 (THF, *C*H_2). Elemental analysis, found C 66.8, H 7.9, N 8.4, cald. For $C_{62}H_{82}Li_3N_6O_8V$ C 66.7, H 7,5, N 8.6.

Synthesis of 5. Freshly sublimed 1,2-diaminobenzene (60 mg, 0.55 mmol) was dissolved in 5 mL of THF. ^{n}BuLi (0.7 mL, 1.6 mol L^{-1} in hexanes, 1.10 mmol) was syringed into this solution dropwise under N_2 at −78 °C, and the solution allowed to warm to room temperature. A solution of Cp_2Ni (100 mg, 0.55 mmol) in 5 mL THF was cooled to −78 °C and the lithiated ligand solution added to this dropwise by syringe. The resulting dark green solution was allowed to warm to room temperature. It was stirred overnight before being while filtered warm. Storage of the filtrate at room temperature afforded highly air-sensitive purple crystals of **5** in a dark green solution. Yield 60 mg, 67% with respect to Cp_2Ni. Melting point, does not melt up to 360 °C. ^{1}H NMR (500.05 MHz, DMSO-d_6), δ (ppm) = 6.45 (6H, d, $^3J_{H-H}$ = 7.58 Hz, H_2), 6.34–6.28 (12H, m, H3–5), 6.32 (6H, d, $^3J_{H-H}$ = 7.58 Hz, H8), 6.14 (6H, t, $^3J_{H-H}$ = 7.58 Hz, H10), 6.08, (6H, t, $^3J_{H-H}$ = 7.58 Hz, H15), 5.76 (6H, t, $^3J_{H-H}$ = 7.58 Hz, H9), 5.65 (6H, d, $^3J_{H-H}$ = 7.58 Hz, H17), 5.55 (6H, t, $^3J_{H-H}$ = 7.58 Hz, H16), 5.51 (H, d, $^3J_{H-H}$ = 7.58 Hz, H11), 5.45 (6H, d, $^3J_{H-H}$ = 7.58 Hz, H14), 3.59 (84H, m, THF CH_2O), 1.75 (84H, m, THF CH_2), 0.63

Table 2 Crystal data for **3–5**

Compound	**3**·2/3PhMe	**4**·2THF	**5**·5THF
Chemical formula	$C_{40.6}H_{23.33}Li_2N_4NiO_4$	$C_{62}H_{82}Li_3N_6O_8V$	$C_{128}H_{181}N_{24}O_{14}Ni_{12}Li_3$
FW	734.80	1111.10	3005.31
Crystal system	Trigonal	Monoclinic	Monoclinic
Space group	$P\bar{3}$	$C2/c$	$P2_1$
a (Å)	20.0120(6)	25.7117(6)	13.2275(3)
b (Å)	20.0120(6)	14.1550(4)	17.0537(7)
c (Å)	8.1348(2)	18.9518(6)	16.5692(6)
α (°)	−90	−90	−90
β (°)	−90	119.140(1)	95.948(3)
γ (°)	−120	−90	−90
V (Å^3)	2821.36(14)	6024.5(3)	3717.5(2)
Z	3	4	1
ρ_{calc} (Mg m^{-3})	1.297	1.225	1.342
μ (Mo-Kα) (mm^{-1})	0.562	0.222	1.543
Reflections collected	15 927	21 086	27 906
Independent reflections (R_{int})	3334 (0.053)	6087 (0.064)	10 066(0.114)
R_1 [$I > 2\sigma(I)$]	0.043	0.069	0.138
wR_2 (all data)	0.114	0.206	0.366

(6H, s, N–H7), 0.58 (6H, s, N–H1), 0.43 (6H, s, N–H6), 0.29 (6H, s, N–H13), −0.05 (6H, s, N–H12), −2.10 (6H, s, N–H18). ^{13}C NMR (125.8 MHz, DMSO-d$_6$), δ (ppm) = 159.4 (*C*18), 158.9 (*C*7), 152.5 (*C*6), 151.0 (C1), 147.9 (*C*12), 146.7 (*C*13), 119.6 (*C*10), 119.6 (*C*15), 119.3 (*C*3, 4), 117.2 (*C*8, 17), 116.6 (*C*5), 116.5 (*C*2), 111.3 (*C*14), 110.5 (*C*11), 109.3 (*C*9), 109.0 (*C*16), 67.1 (THF *C*H$_2$O), 25.2 (THF *C*H$_2$). ^{7}Li NMR (194.4 MHz, DMSO-d$_6$), δ (ppm) = 3.20 (s, 2Li), −1.21 (s, 3Li). Elemental analysis, found C 51.3, H 6.0, N 12.2, cald. for $C_{128}H_{181}N_{24}O_{14}Ni_{12}Li_3$ C 51.2, H 6.1, N 11.2.

X-ray crystallography

Data on **3**·2/3PhMe and **4**·2THF were collected on a Nonius KappaCCD diffractometer equipped with an Oxford cryostream low-temperature device. Crystals were mounted directly from solution using a perfluorohydrocarbon oil that freezes at low temperature.[21] Data were solved by direct methods and refined by full-matrix least squares on F^2.[22] Data for **5** were collected at Beamline I19 of the Diamond Light Source[23] employing silicon double crystal monochromated synchrotron radiation (0.6889 Å) with ω scans at 100(2) K.[24] Data were first treated with ECLIPSE[25] and integration and reduction were undertaken with SAINT and XPREP.[26] A multi-scan empirical absorption correction was applied to the data using SADABS.[26] Crystals of **3**·2/3PhMe contain 2/3 of a molecule of toluene per formula unit, disordered across the −3 positions and refined with constraints. All non-hydrogen atoms were refined anisotropically with the exception of toluene molecules, which were refined isotropically with common thermal parameters per molecule. Crystals of **4**·2THF contain non-coordinated THF molecules which are disordered and these were refined by splitting atoms over two positions. All non-hydrogen atoms were refined anisotropically with the exception of atoms of the disordered THF molecules, which were refined isotropically. The data for **5**·5THF were rather diffuse and of limited resolution due to the superimposition of complexes **5a** and **5b**$^{2-}$. Therefore the data were truncated at 0.92 Å. Ligands and THF molecules in **5** were treated with similar distance and U restraints during the refinement. However, the diffuse character of the electron density did not allow the refinement of disordered atoms over split positions. All atoms were refined isotropically, except Ni atoms which were treated anisotropically. Hydrogen atoms were not considered in the refinement. CCDC 943106–8 contain the supplementary crystallographic data for **3–5**. Details of the data collections and refinements for the compounds are given in Table 2.

Acknowledgements

We thank the UK EPSRC (F. A. S., T. K. R.). We also thank Dr J. E. Davies for collecting X-ray data on **3** and **4** and the Diamond Light Source (UK) for synchrotron beam time on Beamline I19 (MT7569). We thank Dr Julian J. Holstein and Colm Browne for assistance with X-ray data collection for **5**.

Notes and references

1 A. D. Bond, E. A. Harron, R. A. Layfield, C. Soria-Álvarez and D. S. Wright, *Organometallics*, 2001, **20**, 4135; C. Soria-Álvarez, D. Cave, A. D. Bond, E. A. Harron, R. A. Layfield, M. E. G. Mosquera, C. M. Pask, M. McPartlin, J. M. Rawson, P. Wood and D. S. Wright, *Dalton Trans.*, 2003, 3002; F. A. Stokes, R. J. Less, J. Haywood, R. L. Thompson, A. E. H. Wheatley and D. S. Wright, *Organometallics*, 2012, **31**, 23.

2 R. A. Layfield, J. A. McAllister, M. McPartlin, J. M. Rawson and D. S. Wright, *Chem. Commun.*, 2001, 1956; C. Soria-Álvarez, A. Bashall, E. McInnes, R. A. Layfield, M. McPartlin, J. M. Rawson and D. S. Wright, *Chem.–Eur. J.*, 2006, 3053.

3 (*a*) C. Soria-Álvarez, S. R. Boss, J. Burley, S. M. Humphrey, R. A. Layfield, R. A. Kowenicki, M. McPartlin, J. M. Rawson, A. E. H. Wheatley, P. T. Wood and D. S. Wright, *Dalton Trans.*, 2004, 3481; (*b*) C. Brinkmann, F. García, J. V. Moray,

M. McPartlin, S. Singh, A. E. H. Wheatley and D. S. Wright, *Dalton Trans.*, 2007, 1570; (*c*) C. Fernández, F. García, J. V. Morey, M. McPartlin, S. Singh, A. E. H. Wheatley and D. S. Wright, *Angew. Chem., Int. Ed.*, 2007, **46**, 5425; (*d*) J. Haywood, F. A. Stokes, R. J. Less, M. McPartlin, A. E. H. Wheatley and D. S. Wright, *Chem. Commun.*, 2011, **47**, 4120.

4 R. J. Less, V. Naseri, M. McPartlin and D. S. Wright, *Chem. Commun.*, 2011, **47**, 6129.

5 S.-M. Peng and D.-S. Liaw, *Inorg. Chim. Acta*, 1986, **113**, L11; S. K. Brownstein and G. D. Enright, *Acta Crystallogr., Sect. C: Cryst. Struct. Commun.*, 1995, **51**, 1579; S. Stanković and D. Lazar, *Acta Crystallogr., Sect. C: Cryst. Struct. Commun.*, 1995, 51–1581; B. Milliken, L. Borer, M. Russell, M. Bilich and M. M. Olmstead, *Inorg. Chim. Acta*, 2003, **348**, 212.

6 F. A. Stokes, Y. Lv, A. E. H. Wheatley and D. S. Wright, *Chem. Commun.*, 2012, **48**, 11298.

7 Search of the Cambridge crystallography data base, May 2013; Li–N mean 2.08 Å (3312 hits), V–N mean 2.12 Å (2424 hits), Ni–N mean 2.04 Å (14905 hits), Ni–Ni mean 2.61 (range 2.19–3.44) Å (628 hits).

8 For example, L. A. Oro, M. J. Fernandez, J. Modrego, C. Foces-Foces and F. H. Cano, *Angew. Chem., Int. Ed. Engl.*, 1984, **23**, 913; M. J. Jimenez, E. Sola, A. P. Martinez, F. J. Lahoz and L. A. Oro, *Organometallics*, 1999, **18**, 1125.

9 A. J. Blake, M. L. Gillbrand, G. J. Moxey and D. L. Kays, *Inorg. Chem.*, 2009, **48**, 10837.

10 K. W. Helmann, C. Galka, L. H. Gade, A. Steiner, D. S. Wright, T. Kottke and D. Stalke, *Chem. Commun.*, 1998, 549.

11 F. A. Cotton, L. M. Daniels and C. A. Murillo, *Inorg. Chem.*, 1993, **32**, 2881; B. S. Lim, A. Rahtm, J.-S. Park and R. G. Gordon, *Inorg. Chem.*, 2003, **42**, 7951; S. Hao, P. Berno, R. K. Minhas and S. Gambarotta, *Inorg. Chim. Acta*, 1996, **37**, 244; K. R. Gust, J. E. Knox, M. J. Heeg, H. B. Schlegel and C. H. Winter, *Eur. J. Inorg. Chem.*, 2002, 2327.

12 A. Tenten and H. Jacobs, *J. Less-Common Met.*, 1991, **170**, 145.

13 H. G. von Schnering, J.-H. Chang, K. Peters, E.-M. Peters, F. R. Wagner, Y. Grin and G. Thiele, *Z. Anorg. Allg. Chem.*, 2003, **629**, 516.

14 M. S. Paquette and L. F. Dahl, *J. Am. Chem. Soc.*, 1980, **102**, 6621.

15 D. Fenske and J. Ohmer, *Angew. Chem., Int. Ed. Engl.*, 1987, **26**, 148.

16 The pK_a of DMSO is *ca.* 35 (*vs. ca.* 50 for ^{n}BuLi), W. S. Matthews, J. E. Bares, J. E. Bartmess, F. G. Bordwell, F. J. Cornforth, G. E. Drucker, Z. Margolin, R. J. McCallum, G. J. McCollum and N. R. Vanier, *J. Am. Chem. Soc.*, 1975, **97**, 7006.

17 M. J. Frisch, G. W. Trucks, H. B. Schlegel, G. E. Scuseria, M. A. Robb, J. R. Cheeseman, G. Scalmani, V. Barone, B. Mennucci, G. A. Petersson, H. Nakatsuji, M. Caricato, X. Li, H. P. Hratchian, A. F. Izmaylov, J. Bloino, G. Zheng, J. L. Sonnenberg, M. Hada, M. Ehara, K. Toyota, R. Fukuda, J. Hasegawa, M. Ishida, T. Nakajima, Y. Honda, O. Kitao, H. Nakai, T. Vreven, J. A. Montgomery Jr., J. E. Peralta, F. Ogliaro, M. Bearpark, J. J. Heyd, E. Brothers, K. N. Kudin, V. N. Staroverov, R. Kobayashi, J. Normand, K. Raghavachari, A. Rendell, J. C. Burant, S. S. Iyengar, J. Tomasi, M. Cossi, N. Rega, J. M. Millam, M. Klene, J. E. Knox, J. B. Cross, V. Bakken, C. Adamo, J. Jaramillo, R. Gomperts, R. E. Stratmann, O. Yazyev, A. J. Austin, R. Cammi, C. Pomelli, J. W. Ochterski, R. L. Martin, K. Morokuma, V. G. Zakrzewski, G. A. Voth, P. Salvador, J. J. Dannenberg, S. Dapprich, A. D. Daniels, O. Farkas, J. B. Foresman, J. V. Ortiz, J. Cioslowski and D. J. Fox, *Gaussian 09, Revision b.01*, Gaussian, Inc., Wallingford, CT, 2009.

18 Y. Zhao and D. G. Truhlar, *Theor. Chem. Acc.*, 2008, **120**, 215; Y. Zhao and D. G. Truhlar, *Acc. Chem. Res.*, 2008, **4**, 157.

19 C. Floriani and V. Mange, *Inorg. Synth.*, 1990, **28**, 263.

20 E. O. Fischer, *Z. Naturforsch., B: Anorg. Chem. Org. Chem. Biochem. Biophys. Biol.*, 1952, **7**, 377.

21 T. Kottke and D. Stalke, *J. Appl. Crystallogr.*, 1993, **26**, 615.

22 G. M. Sheldrick, *Acta Crystallogr., Sect. A: Fundam. Crystallogr.*, 2008, **64**, 112.

23 H. Nowell, S. A. Barnett, K. E. Christensen, S. J. Teat and D. R. Allan, *J. Synchrotron Radiat.*, 2012, **19**, 435.

24 *Crystalclear*, Rigaku Americas and Rigaku Corporation, TX, USA, 1997–2009.

25 S. Parson, *ECLIPSE*, The University of Edinburgh, Edinburgh, UK, 2004.

26 G. M. Sheldrick, University of Göttingen, Germany, 1996–2008.